ACS OMEGA

http://pubs.acs.org/journal/acsodf

Article

Leaching of Metals from e-Waste: From Its Thermodynamic Analysis and Design to Its Implementation and Optimization

Jose Angel Barragan, Juan Roberto Alemán Castro, Alejandro Aarón Peregrina-Lucano, Moises Sánchez-Amaya, Eligio P. Rivero, and Erika Roxana Larios-Durán*

Cite This: *ACS Omega* 2021, 6, 12063−12071

Read Online

ACCESS | Metrics & More | Article Recommendations

ABSTRACT: The aim of this study is to design and develop an efficient leaching process based on a fundamental and theoretical thermodynamic analysis and the optimization of the operation parameters via the response surface methodology (RSM). Using this methodology, the design of a leaching process for the recovery of copper, silver, and lead from highly metal-concentrated fractions of e-waste is presented. Thermodynamic predictions were performed through the construction and analysis of Pourbaix diagrams for the specific conditions of the leaching system. From this analysis, it was possible to determine the values of potential (E vs NHE) and pH at which the leaching reactions occur spontaneously. Additionally, RSM was useful to deduce a quadratic semiempirical model that predicts the copper leaching efficiencies as a function of two parameters involved in the leaching procedure, the stirring speed and the solid/liquid ratio, by which the response variable, the leaching efficiency, can be optimized.

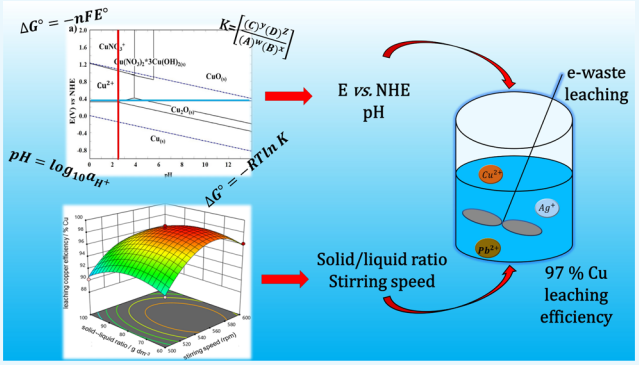

INTRODUCTION

Electronic waste (e-waste) is a municipal solid residue with a major growth rate worldwide in recent years.[1] According to the global e-waste monitor, 53.6 million tons were generated in 2019, expected to increase to 74.7 million tons by 2030.[2] On the other hand, the depletion of natural resources has become a constant problem for the modern society, leading to the search for alternative sources of raw materials. Several methods have been proposed to provide the required material by exploiting secondary resources.[3] In this way, e-waste has attracted attention for its high content in valuable metals, where copper, aluminum, tin, cobalt, and precious metals are the most interesting from an economic point of view.[1]

Although several works have reported pyrometallurgical to hydrometallurgical processes to recover metal values from e-waste, the hydrometallurgical route has been denoted as the most advantageous since it is the more predictable, uses low temperatures, and requires lower investments to its implementation.[4,5]

The majority of the recycling processes of e-waste have adopted traditional methods of size reduction and concentration of values from the mining industry since they have been exhaustively studied and established.[6−10] However, there are yet many points to improve in this procedure. One of the most important and challenging points is to develop a highly selective and efficient metallic leaching procedure that could produce simpler pregnant leaching solutions ready for posterior metal ion recovery. It should be noted that although the leaching processes are a crucial stage in metal recovery processes, the techniques adopted are somewhat empirical[11−14] and only a few works have analyzed the processes from a thermodynamic point of view before their implementation.[15,16] The design of these procedures from a thermodynamic study provides the basis for developing successful processes and reduces the consumption of resources used in research, which is an important subject in practical applications.

This study presents the design of a leaching process of base metals from e-waste, mainly copper, silver, and lead. Nitric acid was selected as the leaching solution since it has reported fast leaching kinetics of the above-mentioned base metals. It has the capability to selectively form stable complexes with the metals of interest but not with other metals that are more economically attractive, such as gold.[17] Thus, the methodology described here would allow establishing a simplified prepurification path to, in subsequent treatment, recover the other more attractive metals

Received: February 8, 2021
Accepted: April 22, 2021
Published: April 30, 2021

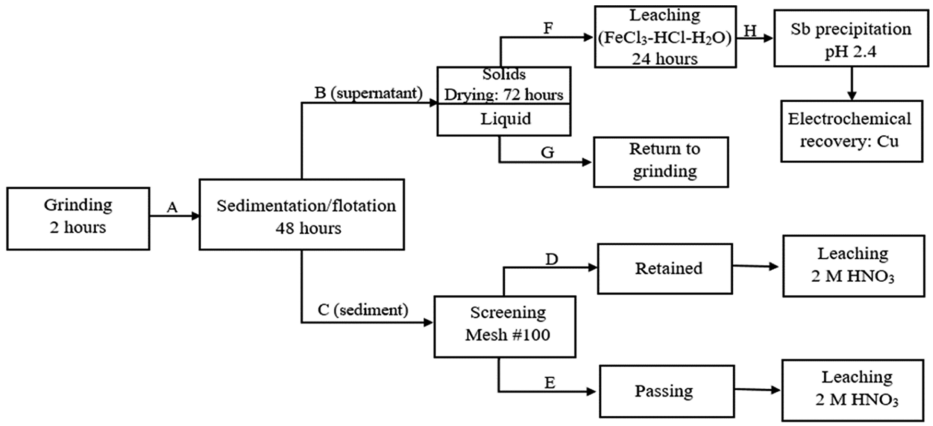

Figure 1. Diagram process for size reduction and concentration of e-waste.[18] Reprinted (adapted) with permission from [*ACS Omega* **2020,** *5,* 21, 12355−12363]. Copyright [2020/American Chemical Society] [ACS Omega/American Chemical Society].

that remain in the solid residue of this leaching step. The subsequent procedure to recover these other metals, such as precious metals, will be reported in future work. Designing copper, silver, and lead follows a simple strategy, including two stages. First, a deep thermodynamic analysis is proposed using Pourbaix diagrams to determine the appropriate and selective parameters employed in the leaching process. Then, as a second step, the procedure of leaching optimization of the operating parameters in a leaching batch reactor via the response surface methodology (RSM) is employed. Two parameters are optimized, namely, the stirring speed and the solid/liquid ratio. Furthermore, it should be noted that the approach presented in this work given by the thermodynamic study of the leaching system and the optimization of the operation parameters of the leaching reactor, which is subjected to the thermodynamic restrictions found, has not been carried out previously. Thus, in-depth analysis and discussion concerning the thermodynamic aspects included in the process and the practical aspects of the optimization parameters are presented.

METHODOLOGY AND MATERIALS

Materials. The e-waste treated in the present work was collected in Guadalajara City. Principally, it was composed of RAM memories and cell phone logic cards. The chemical reagents used in this work were nitric acid (HNO_3, 65%, Golden Bell), hydrochloric acid (HCl, 35%, Golden Bell), hydrogen peroxide (H_2O_2, 50%, Fermont), and distilled water.

Size Reduction and Concentration. According to the process previously established and reported by our research group, a mechanical process for size reduction of the e-waste and concentration of metallic fractions was implemented to treat a highly concentrated metallic material (Figure 1).[18] The main stages of the process consist of wet grinding of e-waste in a ball miller for 2 h, followed by a sedimentation and flotation step (stream A) where two streams in the process were obtained, a supernatant (stream B) and sediment (stream C). The first stream (stream B) had a low percentage of metallic components, and the sediment (stream C) was highly concentrated in metals. The metallic fractions of stream B were treated by lixiviation, followed by the precipitation of Sb and the electrochemical recovery of Cu (streams F and H). This part of the process has already been reported.[18] On the other hand, the highly concentrated material (stream C) was separated into two fractions with a 100-grid sieve; subsequently, streams D and E were obtained. The methodology proposed in this work focuses on designing hydrometallurgical methods and their optimization to recover high metallic contents from streams of this process (D and E). Detailed information and conditions on the mechanical process can be obtained in a previous publication.[18]

Chemical Characterization. To determine the composition of metals in the streams under study, samples of 2 g of e-waste from streams E and D (Figure 1) were leached separately for 2 days. These leaching processes were carried out with aqua regia (HNO_3/3 HCl, V/V) in a solid/liquid ratio of 20 g dm^{-3} with constant magnetic stirrer agitation at room temperature and atmospheric pressure. After leaching, the samples were filtered, and each leached solution was diluted to a volume of 100 dm^{-3} in a volumetric flask. Double dilutions were prepared at 1/10 (V/V) and 1/100 (V/V) dilution factors for posterior analysis by inductively coupled plasma mass spectrometry (ICP−MS, Agilent Technologies 7800). Aqua regia was exclusively used for the chemical characterization purposes detailed in this section. The following leaching methods in the next sections were developed using a nitric acidic solution.

Thermodynamic Study. The thermodynamic study was implemented via Pourbaix diagrams, *E* vs pH, for the metals characterized in Section 2.3 exposed to a leaching system corresponding to 2 mol dm^{-3} HNO_3, which would not apply to those that do not dissolve in nitric acid media, such as gold. All Pourbaix diagrams were constructed with HSC Chemistry 6.0 software for Windows, assuming that the metallic concentration corresponds to the complete dissolution of metals in stream D. It is supposed that this dissolution takes place in a batch leaching reactor operating in a solid/liquid ratio of 100 g dm^{-3} in 0.4 dm^{-3} leaching solution and 2 mol dm^{-3} HNO_3. All diagrams were constructed in terms of the normal hydrogen electrode (NHE).

Leaching Reactor Configuration and Operation. The leaching experiments were performed for 60 min in a 0.5 dm^{-3} glass reactor containing the leaching solution and fitted with a propeller for mechanical agitation. During the leaching process, the pH and potential (*E* vs NHE) were controlled and measured using homemade Arduino project software detailed on website reports.[19] Both potential (*E* vs NHE) and pH values were selected through the Pourbaix diagrams obtained, as described in Section 2.4. Thus, the selected pH was monitored and controlled at a value below 1.2 with the addition of nitric acid (2 mol dm^{-3}), while the potential (*E* vs NHE) remained at a value above 600 mV vs NHE with the addition of H_2O_2 (50%). In this manner, the theoretical information given by the Pourbaix

https://doi.org/10.1021/acsomega.1c00724
ACS Omega 2021, 6, 12063−12071

diagrams to predict efficient and selective metal recovery was experimentally evaluated by the leaching process described here. On the other hand, the temperature reaction was measured as a function of time using a temperature sensor module for Arduino from DF Robot.

Leaching Reactor Optimization by the Response Surface Methodology. The optimized response variable was the leaching copper efficiency achieved in a fixed time of 60 min under the conditions of pH and potential (E vs NHE) predicted by the Pourbaix diagrams and described in Section 2.5. The leaching copper efficiency (ε) was defined as follows

$$\varepsilon = \left[1 - \frac{[M]_f}{[M]_0}\right] \times 100 \quad (1)$$

where $[M]_f$ is the metal composition in the solid residual material of the leaching process and $[M]_0$ is the initial composition for a batch leaching reactor. The characterization of both parameters was performed according to the methodology described in Section 2.3.

Leaching reactor optimization was performed by RSM with a spherical central composite design (CCD)[20] by using Design Expert 12 software for the regression and statistical analysis. The factors of the model were the stirring speed, X_1, and the solid/liquid ratio, X_2, for which the range and levels are shown in Table 1.

Table 1. Variables of the Experimental Design

		range and levels				
codified variable	natural variable	$-\alpha$	-1	0	1	α
X_1	stirring speed (rpm)	479.3	500	550	600	620.7
X_2	solid/liquid ratio (g dm^{-3})	52	60	80	100	108

The number of experiments was defined in agreement with the following expression in eq 2[21]

$$N = 2^K + 2K + n_c \quad (2)$$

where N is the total number of experiments, K is the number of factors in the design, and n_c is the number of central points.[20,21] For this case, two factors were used, and five replicates were applied at the central point of the design.

Process optimization was only developed for the leaching of copper in stream D because according to the process shown in Figure 1 and the characterization of Section 2.3, stream D has the highest concentration of copper. Additionally, copper is significantly more concentrated than the other metals, as will be seen in the following sections. For this reason, it is assumed that the optimal operating conditions for the leaching of copper in stream D produce the complete leaching of the other metals of interest at lower concentrations.

Leaching Test under the Optimized Conditions. Once the optimum conditions of the stirring speed and the solid/liquid ratio in the leaching reactor were defined, the process was implemented for both streams D and E using the optimized point and the pH and potential (E vs NHE) defined by the thermodynamic analysis and the procedure described in Section 2.5. A sample of 2 cm^3 was taken at different periods for chemical characterization by ICP−MS (Agilent Technologies 7800) to determine the time for the maximum leaching rate of every metal in the e-waste and validate the optimization methodology.

RESULTS AND DISCUSSION

Chemical Characterization. Table 2 shows the chemical characterization analysis by ICP−MS of e-waste in streams D and E according to the stream diagram of the process (Figure 1). The results reveal that copper, gold, iron, aluminum, silver, lead, and nickel are present in both streams. As expected, the composition of copper in stream D is 3 times higher than that in stream E. In contrast, for gold, the composition in stream E is 15 times higher than the gold composition in stream D. The characterization done in this section will be used in the thermodynamic analysis of Section 3.2 to determine the concentration expected in the leaching system if a complete dissolution process is obtained.

Thermodynamic Analysis. The thermodynamic analysis performed in terms of the Pourbaix diagrams, E vs pH, is presented in Figure 2 for all the metals coming from stream D, except for gold due to its inability to form stable aqueous complexes and not dissolve in nitric acid media. Pourbaix diagrams were constructed assuming the complete lixiviation of metals, considering the characterization in the previous section (see Table 2) in a solid/liquid ratio of 100 g of e-waste in a volume of 0.4 dm^3 of the leaching solution. Such concentrations correspond to 2.57 M copper, 0.16 mM silver, 9.54 mM lead, 0.24 M iron, 0.32 M aluminum, and 0.24 M nickel.

The thermodynamic parameters, pH and potential (E vs NHE), at which most of the metals in stream D would be leached by 2 mol dm^{-3} HNO_3, are deduced from Figure 2. It is noticeable in the Pourbaix diagram depicted in Figure 2a that to achieve the complete dissolution of copper, the solution potential (E vs NHE) must be higher than 0.35 V vs NHE; otherwise, the dissolution equilibrium is not thermodynamically viable. This thermodynamic restriction is represented in the Pourbaix diagram of Figure 2a with the horizontal blue line. On the other hand, the red line marks the pH value above which the leached copper could precipitate as oxides, $Cu_2O_{(S)}$ or $Cu(NO_3)_2{*}3Cu(OH)2_{(s)}$. Therefore, the copper leaching process must be implemented at a pH below 2.5 to ensure the complete copper dissolution process and avoid any precipitation reaction.

Even though the nitric acid leaching of silver is well known, it is necessary to analyze the thermodynamic feasibility of silver recovery under specific conditions. Figure 2b shows the Pourbaix diagram of silver for stream D at the concentration expected to be reached in a complete dissolution process. From this diagram, it is observed that the dissolution of silver to form Ag^+ or $AgNO_{3(a)}$ is not pH-dependent at least in the range of 0−

Table 2. Multichemical Characterization of Streams D and E by ICP−MS

	metal composition (%)						
stream	Cu	Au	Fe	Al	Ag	Pb	Ni
D	65.550	0.010	5.461	3.452	0.007	0.791	5.672
E	20.165	0.155	2.352	1.560	0.013	0.4253	2.343

https://doi.org/10.1021/acsomega.1c00724
ACS Omega 2021, 6, 12063−12071

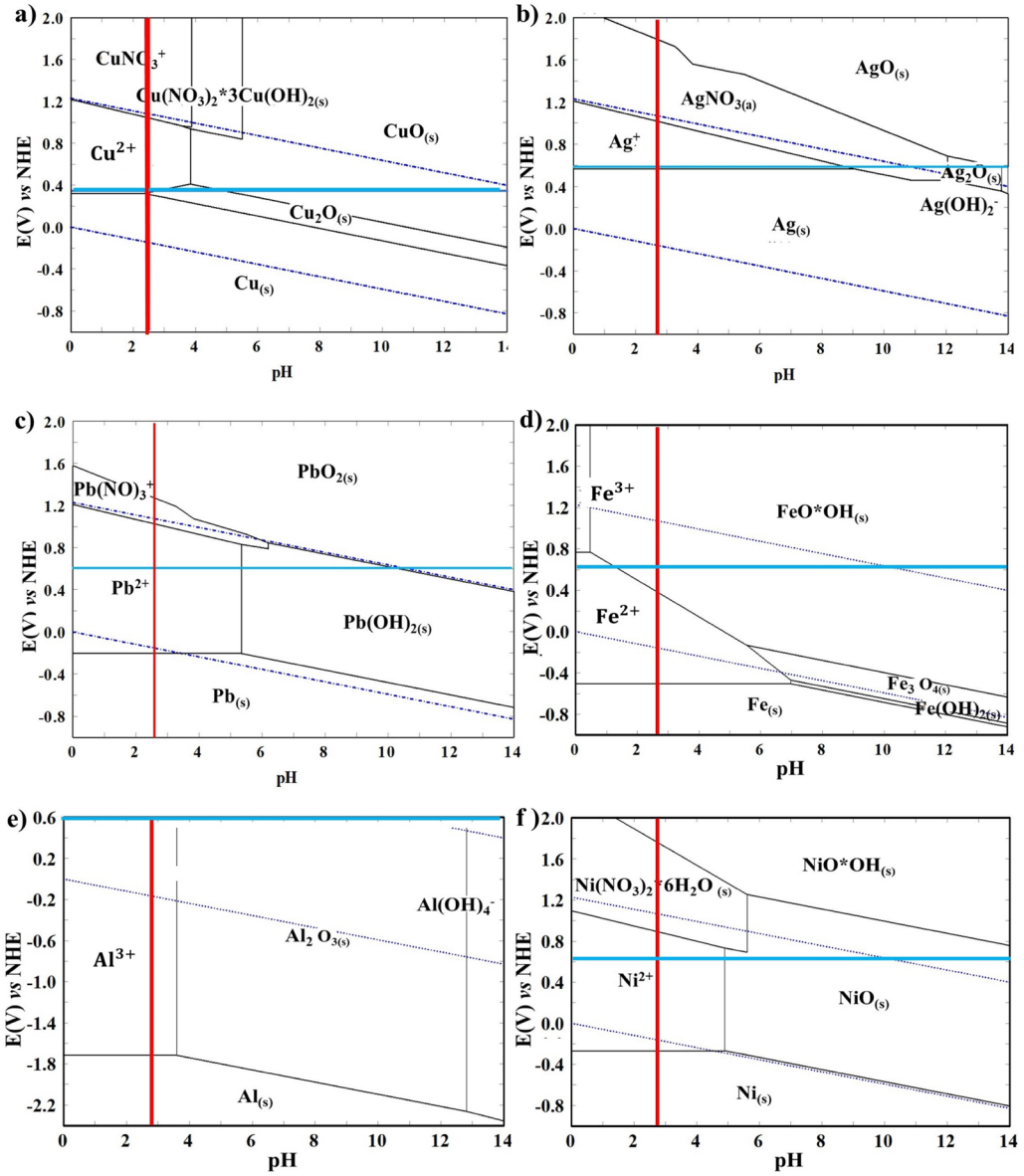

Figure 2. Pourbaix diagrams, E vs pH, of copper in the leaching system. Conditions: 2 mol dm^{-3} HNO_3 as the leaching solution; (a) 2.57 M copper, (b) 0.16 mM silver, (c) 9.54 mM lead, (d) 0.24 M iron, (e) 0.32 M aluminum, and (f) 0.24 M nickel at 25 °C. The red line indicates the pH restriction, and the blue line indicates the potential (*E* vs NHE) restriction for the leaching process.

12. However, the equilibrium between these two chemical species is pH-potential-dependent and the equilibrium between $AgNO_{3(a)}$ and $AgO_{(s)}$, where the passivation process takes place. Nevertheless, the dissolution process of metallic silver to form Ag^+ is potential-dependent and needs to be carried out at potentials greater than 0.6 V vs NHE (see the blue line in Figure 2b). In accordance with the thermodynamic restrictions for copper lixiviation shown in Figure 2a at pH values below 2.5 and potentials greater than 0.35 V vs NHE and the analysis from Figure 2b, silver lixiviation would not take place. To leach both metals, the potential restriction for copper should be modified to 0.6 V vs NHE so that silver can be leached, while the pH restriction could be maintained. Figure 2b shows the modification in the potential value with the blue line, while the red line for pH remains at the same value as in Figure 2a. It is worth noting that although the leaching of silver can be carried out at a higher pH, the modification of this value would compromise the complete leaching of copper.

In the same way, the Pourbaix diagram of lead is presented in Figure 2c, where it is observed that the chemical equilibrium between metallic lead, $Pb_{(s)}$, and Pb^{2+} depends on the potential value, −0.2 V vs NHE, in the range of pH of 0−5.5. Above a pH of 5.5, the leaching of lead is not thermodynamically possible regardless of the potential value, where metallic lead, lead (II) hydroxide, and lead dioxide are present. Thus, a pH value below 2.5 and a potential greater than 0.6 V vs NHE, shown in Figure 2c by the red and blue lines, respectively, predict the complete leaching of not only lead but also copper and silver. Therefore, it is not necessary to modify the pH and potential conditions previously selected. However, it must be considered that if the potential exceeds a value of 1.4 V vs NHE, in the pH range of 0−2.5, lead passivation could occur (see Figure 2c), which is undesirable.

In this way, the leaching of the metals of interest, copper, silver, and lead, presumably reached 0.6 V vs NHE and a pH below 2.5. However, since iron, aluminum, and nickel are

https://doi.org/10.1021/acsomega.1c00724
ACS Omega 2021, 6, 12063−12071

Table 3. ANOVA for the Response Surface Quadratic Empirical Model

source	sum of squares	DF	mean square	*F*-value	P-value	
model	148.71	5	29.74	180.07	<0.0001	significant
X_1	15.47	1	15.47	93.67	<0.0001	significant
X_2	11.97	1	11.97	72.44	<0.0001	significant
X_1X_2	1.00	1	1.00	6.05	0.0434	significant
X_1^2	106.01	1	106.01	641.82	<0.0001	significant
X_2^2	25.88	1	25.88	156.68	<0.0001	significant
residual	1.16	7	0.16			
lack of fit	0.73	3	0.2427	2.27	0.2226	not significant
pure error	0.43	4	0.107			
cor total	149.87	12				
R^2 = 0.9923	$Radj^2$ = 0.9868		$Rpred^2$ = 0.9868		σ = 0.4064	

present in the process and are susceptible to leaching in the nitric acid medium, it is necessary to carry out their thermodynamic analysis by the same route. These results are presented in Figure 2d−f, respectively. For iron (Figure 2d), three chemical species are present in the region of interest, with a potential greater than 0.6 V vs NHE and a pH below 2.5, Fe^{2+}, Fe^{3+}, and $FeO^*OH_{(s)}$. As can be observed, partial dissolution of iron takes place under these pH and potential conditions. The leaching of iron is favored if the pH is modified to more acidic values. The potential is not a major concern for the leaching of iron since the equilibrium between Fe and Fe^{2+} occurs at a thermodynamic potential of −0.4 V vs NHE. In fact, a lower potential value than the previously chosen 0.6 V vs NHE favors the pH range in which Fe^{2+} is stable in this medium. Similarly, the Pourbaix diagram for aluminum was generated and is presented in Figure 2e. As aluminum is a more active metal in the galvanic series, the thermodynamic equilibrium between metallic aluminum, $Al_{(s)}$, and Al^{3+} is found at a potential value of −1.7 V vs NHE and a pH range of 0−3.8. In the pH range of 4−13, the passivation process of aluminum takes place by the formation of $Al_2O_{3(s)}$. Through the descriptions of Figure 2e and the restrictions of the leaching of copper, silver, and lead, it is expected that the aluminum present in stream D would be leached under these conditions. Finally, the nickel Pourbaix diagram is presented in Figure 2f. The most relevant information, in this case, is the equilibrium between metallic $Ni_{(s)}$ and Ni^{2+} given at a potential of −0.3 V vs NHE and in a pH range of 0−5. Above this pH range, the passivation zone of nickel is present by the formation of $NiO_{(s)}$ and $NiO^*OH_{(s)}$. According to the working leaching conditions for copper, silver, and lead, which are marked in the nickel Pourbaix diagram by the blue and red lines for the potential and pH, respectively, the leaching of nickel takes place as long as the potential value does not exceed 0.85 V vs NHE, where the precipitation of Ni^{2+} to $Ni(NO_3)_2{\cdot}6H_2O$ is plausible.

Therefore, the variables of pH and potential (E vs NHE) for the leaching process of copper, silver, and lead in 2 mol dm^{-3} nitric acid media are now defined and established as thermodynamic restrictions by the analysis of Pourbaix diagrams. These parameters correspond to a pH below 2.5 and a potential greater than 0.6 V vs NHE. Furthermore, at these parameters it is expected to leach, completely or partially, other metals present in the e-waste from stream D, such as iron, aluminum, and nickel. The validity of the thermodynamic information obtained by the Pourbaix diagrams should be corroborated in the leaching tests. The thermodynamic parameters for implementing the leaching process should not be modified or studied from another point of view since it has been demonstrated that the leaching process is only spontaneous under the thermodynamic conditions established in this study. Therefore, experimenting under different conditions does not make sense because the process will not occur or will take place partially. In this manner, if copper, silver, and lead are the metals of interest to be leached, the leaching process must be strictly implemented at a pH value equal to or below 2.5 and a potential range between 0.6 and 1.4 V vs NHE. These conditions are favorable for equal or lower concentrations of the metallic fractions treated in this work and the leaching system studied here. If leaching of other metals or higher metallic concentrations is desired, modification of the Pourbaix diagrams and, consequently, the leaching conditions should be considered.

It is worth noting that this study only takes into account the thermodynamic viability of the process but not the kinetics of the reactions, for which complementary investigation would be required to establish the kinetics law related the specific time at which complete leaching would take place.

Optimization RSM. The process variables, namely, the stirring speed and the solid/liquid ratio, are optimized in the leaching reactor as described in Section 2.6. For this purpose, RSM was implemented with Design Expert 12 software for Windows, and the semiempirical second-order model presented in eq 3 was obtained for the leaching of copper in terms of codified variables

$$Y = 98.62 + 1.39X_1 - 1.22X_2 - 0.5X_1X_2 - 3.9{X_1}^2 - 1.93{X_2}^2 \quad (3)$$

where Y is the codified response variable, named leaching efficiency, ε, and defined in eq 1, while X_1 and X_2 are the stirring speed and the solid/liquid ratio, respectively, as defined in Table 1. From the semiempirical model obtained, the optimization process can be developed from its mathematical or graphic analysis. In accordance with RSM, a graphical optimization was performed in this work and is discussed later in this section.

Table 3 presents the analysis of variance (ANOVA) results of the fitted model, with a significance level of 95%. ANOVA indicates that the polynomial second-order model is significant and adequately predicts the leaching efficiency. The input variables X_1 and X_2 are significant in all their terms, linear, quadratic, and interactions (p-value < 0.05). The lack of fit was not significant, as expected. Furthermore, the model is verified by the regression coefficient, where the values of R^2 and $Radj^2$ are 0.9923 and 0.9868, respectively. Since an adequate value of the regression coefficients is above 0.9,[20] the model described by eq 3 predicts the response variable accurately.

https://doi.org/10.1021/acsomega.1c00724
ACS Omega 2021, 6, 12063−12071

The actual values of leaching efficiency versus the values predicted by the quadratic model given in eq 3 are shown in Figure 3, from which the adequate fit of the predicted values to

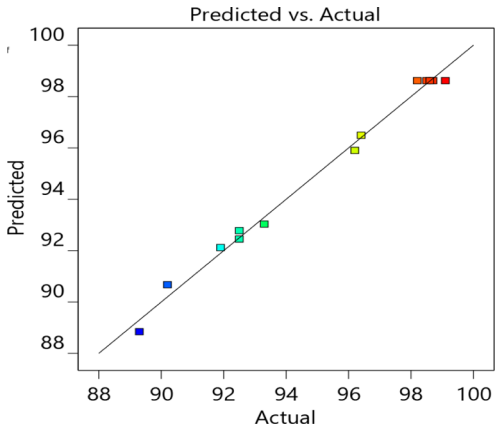

Figure 3. Actual values of the leaching efficiency (experimental) *vs* values predicted by the response surface quadratic model.

the experimental data is evident. This agrees with the similarity of the numerical values of the regression coefficients, R^2, R_{adj}^2, and R_{pred}^2, reported in Table 3. Furthermore, a value of 0.4064 is reported for the standard deviation σ, which indicates that small differences between the predicted and actual values are obtained.

Figure 4 shows the response surface of the leaching copper efficiency as a function of the solid/liquid ratio and the stirring

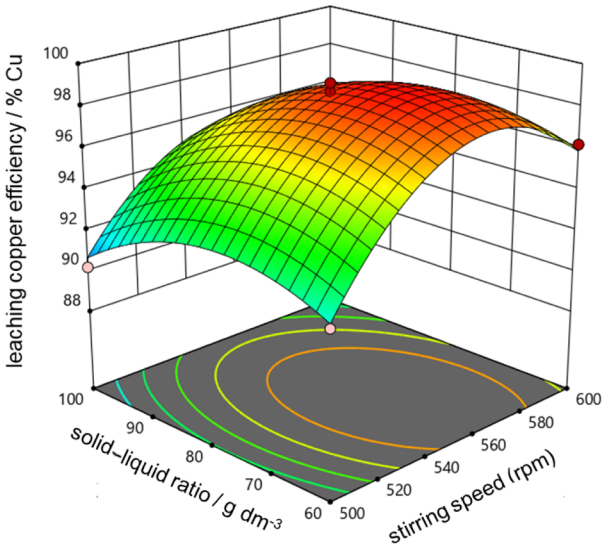

Figure 4. Response surface of the leaching copper efficiency vs solid/liquid ratio (g dm^{-3}) and stirring speed (rpm).

speed, and the isoresponse curves. The response surface is a prediction of the leaching copper efficiency by the second-order empirical model deduced in this work and reported in eq 3. A graphical analysis of Figure 4 allows predicting the leaching copper efficiency at different solid/liquid ratios and stirring speeds as the operating conditions. As observed in Figure 4, high leaching copper efficiencies, between 96 and 98%, could be obtained if the processes are operated in the ranges of the internal isoresponse, indicated by the orange curve. Nevertheless, even when these efficiencies are acceptable from a graphical analysis and a mathematical point of view, from a practical and operational perspective, the appropriate conditions are those that require the lowest energy consumption at the highest solid/liquid ratio.

In this sense, the selected operating conditions were a 540 rpm stirring speed and an 80 g dm^{-3} solid/liquid ratio. According to the response surface from Figure 4, when these conditions are imposed at the batch leaching reactor, the process produces copper leaching efficiencies above 96% at the lowest possible stirring speed and the highest solid/liquid ratio, achieving the expected efficiency in 60 min of operation. These operating conditions would guarantee high leaching efficiencies at low energy consumption. On the other hand, selecting the highest possible solid/liquid ratio produces a more concentrated leaching pregnant solution, which would allow us to obtain the highest efficiencies in the posterior recuperation processes.

Leaching Test under the Optimized Conditions. After the analysis above-exposed, the leaching process was implemented to determine the exact leaching time for each metallic component. Even when the thermodynamic and statistical analysis was developed for stream D, the leaching process was carried out in both streams D and E to analyze the effect of the variability of the metallic composition.

Figure 5 shows the variability of the metallic concentration as a time function at different periods of the leaching process for stream D. Figure 5a shows the concentration behavior for copper, nickel, and copper in g dm^{-3}, while Figure 5b shows the response for lead, silver, aluminum, and gold in mg dm^{-3}. According to Figure 5a, at a leaching time of approximately 50 min, copper reaches its maximum concentration, 65 g dm^{-3}, corresponding to 97% of the initial copper composition in the e-waste. After this time, the copper concentration remained constant, and no precipitation reactions took place. This fact was due to the control of the thermodynamic parameters, pH and potential (E vs NHE), which remained in the range of the values selected from the Pourbaix diagram analysis shown in Figure 2 (pH < 1.2, E > 600 mV vs NHE). Figure 5c shows the behavior of these parameters as a function of the leaching time, where the noticeable increments of both parameters depict the automatic addition of nitric acid and H_2O_2 to control the value of the pH and potential (E vs NHE), respectively.

On the other hand, the nickel and iron concentrations were lower than those of copper, 4 and 6 g dm^{-3}, respectively, and remained constant after 30 min of leaching time. The iron concentration shows some instabilities since the conditions used are not completely viable for its lixiviation.

The concentration behavior of lead, silver, aluminum, and gold as a time function is shown in Figure 5b. Even when gold leaching was unexpected, its presence and detection by ICP–MS analysis could be due to impurities in the leaching system as well as in the e-waste, where some other agents could dissolve and form complexes with a low fraction of gold. However, as noticed, the concentration of gold is almost negligible, reaching 5 mg dm^{-3} and remaining constant during the entire process.

As observed in Figure 5b, the silver concentration reaches its maximum value, 200 mg dm^{-3}, after 20 min of leaching, while the lead and aluminum concentrations reach their maximum values at 30 min, which tend to decrease at longer times until attaining more stable values of 300 and 100 mg dm^{-3}, respectively, after 60 min. This phenomenon would be related to thermodynamic nonidealities, such as the ionic interactions that modified the activity coefficients. As shown in Figure 5c, the

https://doi.org/10.1021/acsomega.1c00724
ACS Omega 2021, 6, 12063−12071

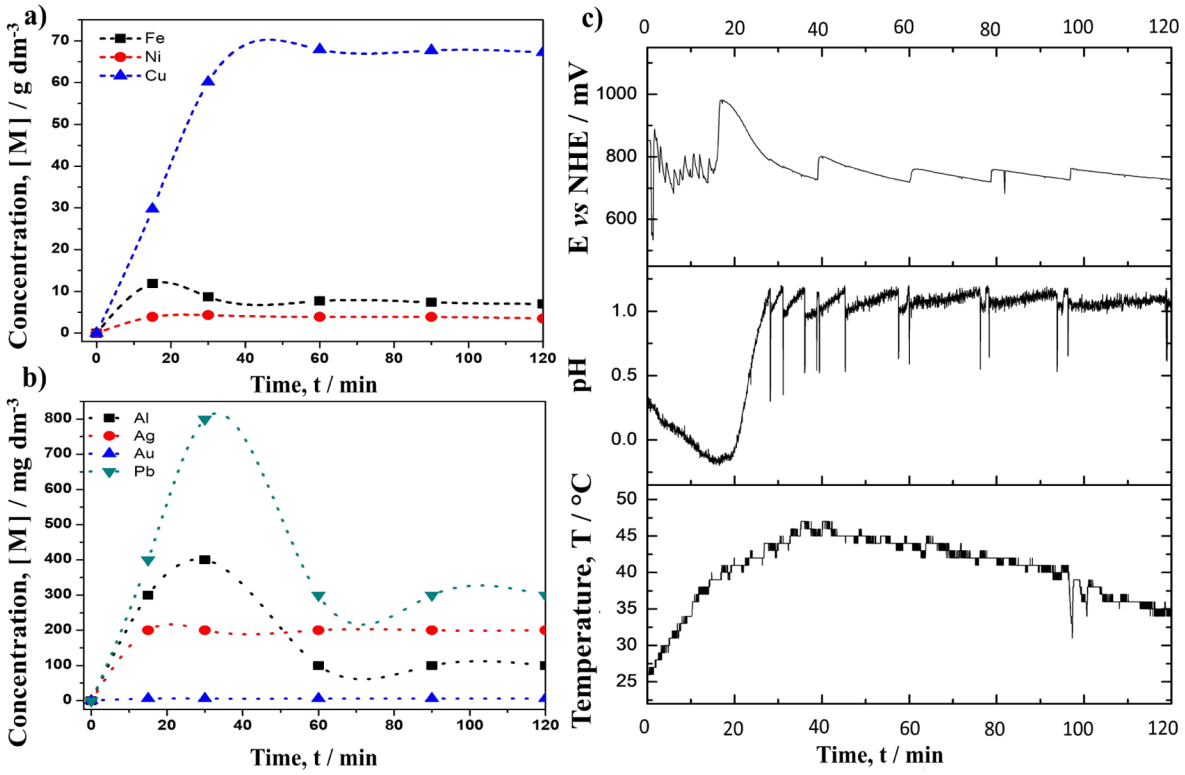

Figure 5. Leaching test of stream D at the optimized parameters in the leaching reactor and the thermodynamic restrictions. Conditions: e-waste stream D; nitric acid concentration: 2 mol dm^{-3}; stirring speed: 540 rpm; solid/liquid ratio: 80 g dm^{-3}. (a) Concentration of Fe, Ni, and Cu vs time. (b) Concentration of Al, Ag, Pb, and Au vs time. (c) *E* vs NHE; pH and temperature vs time.

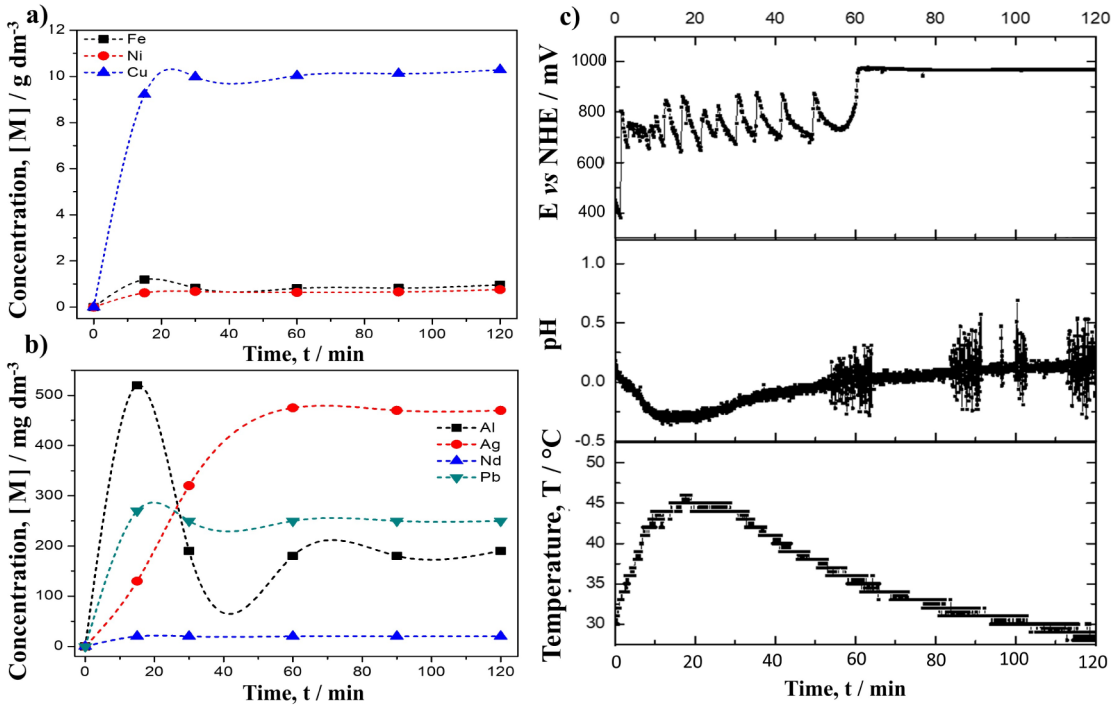

Figure 6. Leaching test of stream E at the optimized parameters in the leaching reactor and the thermodynamic restrictions. Conditions: e-waste stream E; nitric acid concentration: 2 mol dm^{-3}; stirring speed: 540 rpm; solid/liquid ratio: 80 g dm^{-3}. (a) Concentration of Fe, Ni, and Cu vs time. (b) Concentration of Al, Ag, Pb, and Nd vs time. (c) *E* vs NHE; pH and temperature vs time.

homemade Arduino program adequately controlled the leaching parameters, ensuring pH values of approximately 1, while the potential was controlled at approximately 1000 and 700 mV versus NHE, for which 5 cm^3 of H_2O_2 was used in the process. The perturbations in the data reported in Figure 5c for the potential and pH measurements correspond to the addition of

https://doi.org/10.1021/acsomega.1c00724
ACS Omega 2021, 6, 12063−12071

reagents for parameter control. Moreover, the temperature monitored during the experiments shows that the leaching of these metals is an exothermic process.

The leaching process conditions established and developed for stream D were tested in stream E, and the results are reported in Figure 6. Figure 6a shows that the maximum copper concentration corresponding to 10 g dm^{-3} was achieved in 20 min of operation; after this time, the concentration remained constant. In addition to the previous process, stream D (Figure 5), iron, and nickel were also leached at lower concentrations than copper but higher concentrations than the other metals leached in the process; both reached similar concentrations, approximately 1 g dm^{-3} at 30 min of leaching.

On the other hand, the silver concentration corresponds to 450 g dm^{-3} at 60 min of operation, while lead reaches 240 g dm^{-3} and aluminum reaches 200 mg dm^{-3} at 30 min, as observed in Figure 6b. The lead concentration behavior is more stable than that observed in the leaching of stream D, while the aluminum concentration tendency is similar to that previously observed in Figure 5b. No gold concentration is reported in stream E; however, neodymium is obtained at a constant concentration of 25 g dm^{-3}.

Controlling the potential (E vs NHE) is more difficult in stream E than in stream D, especially in the first 60 min of operation where the leaching reaction takes place. Thus, a greater number of additions of H_2O_2 are required in this case, as shown in Figure 6c. In this manner, 8 cm^{-3} H_2O_2 was required to maintain the potential above 600 mV vs NHE. However, after 60 min, the potential (E vs NHE) attains a constant value, indicating that the leaching reactions have ended, which is in good agreement with the concentration behavior observed in Figure 6a,b. On the other hand, the pH had a more stable behavior, and no nitric acid additions were needed to control it.

In addition to stream D, the temperature values reveal an exothermic process, and higher increments are obtained at the beginning of the process where the leaching reaction occurs.

In this way, according to the results obtained in this section, it is verified that the conditions defined in the thermodynamic study, pH and potential (E vs NHE), as well as the operating parameters of the leaching reactor, solid/liquid ratio and stirring speed optimized by RSM, conform to the most suitable strategy for the design of efficient leaching processes. Furthermore, the expected concentrations of metal ions at the end of the process can be predicted in relatively short times. Therefore, it is recommended to follow the same methodology in designing new and complete leaching processes.

CONCLUSIONS

The leaching process of copper, lead, and silver was successfully implemented by its design based on a thermodynamic study that deduced its optimal parameters, pH below 2.5 and potentials greater than 0.6 V vs NHE, for the efficient leaching in nitric acid media, 2 mol dm^{-3} HNO_3. Carrying out the thermodynamic study and monitoring and controlling the pH and the potential at a constant value during the leaching time were fundamental keys to the success of the process.

RSM is envisioned as a powerful tool for optimizing process parameters in a batch leaching reactor. Under this methodology, a semiempirical quadratic model was obtained, which predicts the leaching efficiency of copper in the region of study at different stirring speeds and solid/liquid ratios.

Under the combination of both techniques, an efficient leaching process was developed, through which a high leaching efficiency was obtained. This approach had not been previously reported.

In summary, a 97% copper efficiency and the complete leaching of silver and lead from high-concentrated metal fractions of e-waste in both streams, D and E, were obtained. This methodology could be applied in the leaching of other metals from different sources.

A robust model by RSM will be developed in the future to validate the leaching efficiencies under a wide range of initial metal concentrations in e-waste.

AUTHOR INFORMATION

Corresponding Author

Erika Roxana Larios-Durán − *Departamento de Ingeniería Química, Universidad de Guadalajara, C.P. 44430 Guadalajara, Jalisco, Mexico*; orcid.org/0000-0002-0945-3546; Phone: +52 33 13785900, ext 27515; Email: erika.lduran@academicos.udg.mx

Authors

Jose Angel Barragan − *Departamento de Ingeniería Química, Universidad de Guadalajara, C.P. 44430 Guadalajara, Jalisco, Mexico*

Juan Roberto Alemán Castro − *Departamento de Ingeniería Química, Universidad de Guadalajara, C.P. 44430 Guadalajara, Jalisco, Mexico*

Alejandro Aarón Peregrina-Lucano − *Departamento de Farmacobiología, Universidad de Guadalajara, C.P. 44430 Guadalajara, Jalisco, Mexico*

Moises Sánchez-Amaya − *Departamento de Ingeniería Química, Universidad de Guadalajara, C.P. 44430 Guadalajara, Jalisco, Mexico*

Eligio P. Rivero − *Facultad de Estudios Superiores Cuautitlán, Departamento de Ingeniería y Tecnología, Universidad Nacional Autónoma de México, Cuautitlán Izcalli, Estado de México 54740, Mexico*

Complete contact information is available at: https://pubs.acs.org/10.1021/acsomega.1c00724

Notes

The authors declare no competing financial interest.

ACKNOWLEDGMENTS

J.A.B. and M.S.-A. are grateful to CONACyT for financial support for their Ph.D. studies.

ABBREVIATIONS

RAM	random access memories
RSM	response surface methodology
CCD	central composite design
NHE	Normal hydrogen electrode
WPCBs	waste printed circuit boards

SYMBOLS

E	leaching copper efficiency
$[M]_f$	final metal composition
$[M]_0$	initial metal composition
N	number of experiments
K	design factors
M	molecular weight
n_c	number of central points
R^2	coefficient of determination

https://doi.org/10.1021/acsomega.1c00724
ACS Omega 2021, 6, 12063−12071

$Radj^2$	adjusted coefficient of determination
$Rpred^2$	predicted coefficient of determination
σ	standard deviation

REFERENCES

(1) Cucchiella, F.; D'Adamo, I.; Lenny Koh, S. C.; Rosa, P. Recycling of WEEEs: An economic assessment of present and future e-waste streams. *Renew. Sustain. Energy Rev.* **2015**, *51*, 263−272.

(2) Forti, V.; Baldé, C. P.; Kuehr, R.; Bel, G. *The Global E-Waste Monitor 2020: Quantities, Streams, and the Circular Economy Potential*; United Nations University, 2020.

(3) European Commission. *Communication from the Commission—Towards a Circular Economy: A Zero Waste Programme for Europe*; European Commission, 2014; Vol. *398*, pp 1−14. https://ec.europa.eu/environment/circular-economy/pdf/circular-economy-communication.pdf.

(4) Bhat, V.; Rao, P.; Patil, Y. Development of an Integrated Model to Recover Precious Metals from Electronic Scrap - A Novel Strategy for E-Waste Management. *Procedia Soc. Behav. Sci.* **2012**, *37*, 397−406.

(5) Birloaga, I.; Coman, V.; Kopacek, B.; Vegliò, F. An advanced study on the hydrometallurgical processing of waste computer printed circuit boards to extract their valuable content of metals. *Waste Manag.* **2014**, *34*, 2581−2586.

(6) Tesfaye, F.; Lindberg, D.; Hamuyuni, J.; Taskinen, P.; Hupa, L. Improving urban mining practices for optimal recovery of resources from e-waste. *Miner. Eng.* **2017**, *111*, 209−221.

(7) Sarvar, M.; Salarirad, M. M.; Shabani, M. A. Characterization and mechanical separation of metals from computer Printed Circuit Boards (PCBs) based on mineral processing methods. *Waste Manag.* **2015**, *45*, 246−257.

(8) Kumar, V.; Lee, J.-c.; Jeong, J.; Jha, M. K.; Kim, B.-s.; Singh, R. Novel physical separation process for eco-friendly recycling of rare and valuable metals from end-of-life DVD-PCBs. *Sep. Purif. Technol.* **2013**, *111*, 145−154.

(9) Zhao, C.; Zhang, X.; Ding, J.; Zhu, Y. Study on recovery of valuable metals from waste mobile phone PCB particles using liquid-solid fluidization technique. *Chem. Eng. J.* **2017**, *311*, 217−226.

(10) He, J.; Duan, C. Recovery of metallic concentrations from waste printed circuit boards via reverse floatation. *Waste Manag.* **2017**, *60*, 618−628.

(11) Jadhao, P.; Chauhan, G.; Pant, K. K.; Nigam, K. D. P. Greener approach for the extraction of copper metal from electronic waste. *Waste Manag.* **2016**, *57*, 102−112.

(12) Yang, X.; Moats, M. S.; Miller, J. D.; Wang, X.; Shi, X.; Xu, H. Thiourea-thiocyanate leaching system for gold. *Hydrometallurgy* **2011**, *106*, 58−63.

(13) Yang, H.; Liu, J.; Yang, J. Leaching copper from shredded particles of waste printed circuit boards. *J. Hazard. Mater.* **2011**, *187*, 393−400.

(14) Chen, M.; Zhang, S.; Huang, J.; Chen, H. Lead during the leaching process of copper from waste printed circuit boards by five typical ionic liquid acids. *J. Clean. Prod.* **2015**, *95*, 142−147.

(15) Torres, R.; Lapidus, G. T. Copper leaching from electronic waste for the improvement of gold recycling. *Waste Manag.* **2016**, *57*, 131−139.

(16) Liu, X.; Xu, B.; Yang, Y.; Li, Q.; Jiang, T.; He, Y. Thermodynamic analysis of ammoniacal thiosulphate leaching of gold catalysed by Co(III)/Co(II) using Eh-pH and speciation diagrams. *Hydrometallurgy* **2018**, *178*, 240−249.

(17) Ajiboye, E. A.; Panda, P. K.; Adebayo, A. O.; Ajayi, O. O.; Tripathy, B. C.; Ghosh, M. K.; Basu, S. Leaching kinetics of Cu, Ni and Zn from waste silica rich integrated circuits using mild nitric acid. *Hydrometallurgy* **2019**, *188*, 161−168.

(18) Barragan, J. A.; de León, C. P.; Castro, J. R. A.; Peregrina-Lucano, A.; Gómez-Zamudio, F.; Larios-Durán, E. R. Copper and Antimony Recovery from Electronic Waste by Hydrometallurgical and Electrochemical Techniques. *ACS Omega* **2020**, *5*, 12355−12363.

(19) DJalexander1021. pH Regulater/Meter—Arduino. Published 2017. https://www.instructables.com/member/DJalexander1021/ (accessed August 29th 2018).

(20) Myers, R. H.; Montgomery, D. C.; Anderson-Cook, C. M. *Response Surface Methodology: Process and Product Optimization Using Designed Experiments*; John Wiley & Sons, 2011.

(21) Montgomery, D. C. *Diseño y Analisis de Experimentos*, Segunda ed.; Limusa Wiley, 2004.

https://doi.org/10.1021/acsomega.1c00724
ACS Omega 2021, 6, 12063−12071